

Steady-State Voltammetry of Hydroxide Ion Oxidation in Aqueous Solutions Containing Ammonia

Salvatore Daniele,* M. Antonietta Baldo, and Carlo Bragato

Department of Physical Chemistry, University of Venice, Calle Larga S. Marta, 2137, 30123 Venice, Italy

Mamdouh Elsayed Abdelsalam and Guy Denuault

Department of Chemistry, The University of Southampton, S017 -1BJ, Southampton, U.K.

An oxidation process observed in dilute aqueous solutions of ammonia was investigated under steady-state conditions with gold microelectrodes with radii in the range 2.5–30 μm . Over the ammonia concentration range 0.1–10 mM, a well-defined voltammetric wave was observed at ~ 1.4 V versus Ag/AgCl. It was attributed to the oxidation of hydroxide ions that arise from the dissociation of the weak base. The steady-state limiting current was found to depend on the concentration of supporting electrolyte, and in solution with low electrolyte, it was enhanced by migration contribution, as expected for a negatively charged species that oxidizes on a positively charged electrode. In addition, the steady-state limiting current was proportional to both the ammonia concentration and the electrode radius. The overall electrode process was analyzed in terms of a CE mechanism (homogeneous chemical reaction preceding the heterogeneous electron transfer) with a fast chemical reaction when measurements were carried out in solutions containing NH_3 at ≤ 5 mM and with electrodes having a radius of ≥ 5 μm . This was ascertained by comparing experimental and theoretical data obtained by simulation. The formation of the soluble complex species $\text{Au}(\text{NH}_3)_2^+$ was also considered as a possible alternative to explain the presence of the oxidation wave. This process however was ruled out, as the experimental data did not fit theoretical predictions in any of the conditions employed in the investigation. Instead, the direct oxidation of NH_3 , probably to N_2O , was invoked to explain the anomalous currents found when the CE process was strongly kinetically hindered. Throughout this study, a parallel was made between the CE mechanism investigated here and that known to occur during the hydrogen evolution reaction from weak acids.

In the latter decade, voltammetric and amperometric approaches under steady-state conditions have been investigated to develop nonpotentiometric routes for the determination of acid or base concentrations in aqueous solutions.^{1–15} It has been shown that the concentration of either strong or weak acids can be determined by exploiting the reduction process of hydrogen ions at platinum microelectrodes.^{1–9,12–14} Similarly, the concentration

of strong bases can be determined by exploiting the oxidation process of hydroxide ions at gold microelectrodes.^{10,11,15} Weak acids produce reduction waves that involve a CE mechanism^{6,9} (homogeneous chemical reaction preceding the hydrogen ion reduction at the electrode). In this context, the voltammetric behavior of weak bases in aqueous solution has not been examined yet, although in principle, a wave for hydroxide ions oxidation should also be observed in their dilute aqueous solutions. By analogy with the behavior observed for the hydrogen evolution reaction from weak acids, the oxidation process of a weak base (B), via the hydroxide ion oxidation, should involve a CE mechanism:

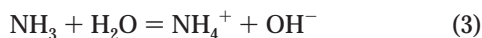


However, we are unaware of papers reporting on such a mecha-

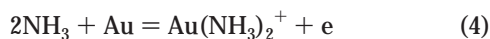
- (1) Ciszowska, M.; Stojek, Z.; Morris, S. E.; Osteryoung, J. G. *Anal. Chem.* **1992**, *64*, 2372–2377.
- (2) Troise Frank, M. H.; Denuault, G. *J. Electroanal. Chem.* **1993**, *354*, 331–339.
- (3) Stojek, Z.; Ciszowska, M.; Osteryoung, J. G. *Anal. Chem.* **1994**, *66*, 1507–1512.
- (4) Ciszowska, M.; Stojek, Z.; Osteryoung, J. G. *J. Electroanal. Chem.* **1995**, *398*, 49–56.
- (5) Perdicakis, M.; Piatnicki, C.; Sadik, M.; Pasturaud, R.; Benzakour, B.; Bessiere, J. *Anal. Chim. Acta* **1993**, *273*, 81–91.
- (6) Daniele, S.; Lavagnini, I.; Baldo, M. A.; Magno, F. *J. Electroanal. Chem.* **1996**, *404*, 105–111.
- (7) Daniele, S.; Baldo, M. A.; Simonetto, F. *Anal. Chim. Acta* **1996**, *331*, 117–123.
- (8) Ciszowska, M.; Jaworski, A.; Osteryoung, J. G. *J. Electroanal. Chem.* **1997**, *423*, 95–101.
- (9) Daniele, S.; Lavagnini, I.; Baldo, M. A.; Magno, F. *Anal. Chem.* **1998**, *70*, 285–294.
- (10) Abdelsalam, M. E.; Denuault, G.; Baldo, M. A.; Daniele, S. *J. Electroanal. Chem.* **1998**, *449*, 5–7.
- (11) Daniele, S.; Baldo, M. A.; Bragato, C.; Denuault, G.; Elsayed Abdelsalam, M. *Anal. Chem.* **1999**, *71*, 811–818.
- (12) Daniele, S.; Baldo, M. A.; Bragato, C.; Lavagnini, I. *Anal. Chim. Acta* **1998**, *361*, 141–150.
- (13) Baldo, M. A.; Daniele, S.; Bragato, C.; Mazzocchin, G. A. *Analyst* **1999**, *124*, 1059–1063.
- (14) Baldo, M. A.; Daniele, S.; Bragato, C.; Mazzocchin, G. A. *Electroanalysis* **2001**, *13*, 737–743.
- (15) Abdelsalam, M. E.; Denuault, G.; Baldo, M. A.; Bragato, C.; Daniele, S. *Electroanalysis* **2001**, *13*, 289–294.

nism for weak bases. To address this problem we have undertaken a series of investigations concerning the anodization of gold microelectrodes in aqueous solutions containing weak bases. Because of its environmental and biological importance, ammonia has been considered first.

In aqueous solution, ammonia undergoes the following acid–base equilibrium:



and the base dissociation constant K_b is equal to 1.75×10^{-5} at zero ionic strength.¹⁶ Thus, dilute solutions of ammonia should provide concentrations of OH^- large enough to yield a significant oxidation wave. This scenario, however, could be complicated by the direct oxidation of ammonia itself. Direct electrochemical oxidation of ammonia in aqueous solution has been found to occur on several metals such as platinum, iridium, rhodium, and palladium¹⁷ or metal oxide-coated electrodes.¹⁸ On conventional gold electrodes, an oxidation wave has also been observed in solutions containing relatively large concentrations of ammonia (≥ 0.1 M). In this case, however, the electrode process is thought to be mainly due to the electrodisolution of gold to form a gold–ammonia complex:^{19,20}



This article seeks to verify whether or to what extent the anodization of gold microelectrodes in dilute ammonia solutions provides an oxidation wave that involves the CE mechanism via the route 1–2. To address these questions, measurements were carried out with different-size gold microdisk electrodes in several aqueous solutions containing a range of ammonia concentrations. Measurements were also carried out with no deliberately added and with small concentrations of supporting electrolyte to assess whether migration contributes to the mass transport and consequently to establish whether electroactive species bearing a charge are involved in the electrode process. To elucidate which mechanism applies, experimental steady-state limiting currents were also compared with theoretical predictions. Finally, the analytical usefulness of oxidation waves involving ammonia is addressed.

EXPERIMENTAL SECTION

All the chemicals employed were of analytical-reagent grade. All the aqueous solutions were prepared with freshly boiled Milli-Q water stored under a nitrogen atmosphere. Carbonate-free 0.1 M ammonia and sodium hydroxide solutions were stored in polythene bottles and maintained under a nitrogen atmosphere. The absence of carbonate in the solutions was tested daily as described

elsewhere.¹¹ All the basic solutions were standardized by acid–base titrations.

The background electrolyte concentration was estimated from conductivity measurements as described elsewhere.¹¹ The conductivity of pure deaerated water ranged between 0.6 and $2 \mu\text{S cm}^{-1}$. These yielded a background concentration of electrolyte expressed as KCl over the range 4–14 μM .

Unless otherwise stated, the measurements were carried out at room temperature after deoxygenating the solutions with a stream of water-saturated CO_2 -free nitrogen.

Voltammetric experiments with microelectrodes were carried out in a two-electrode cell located in a Faraday cage made of aluminum sheets. Unless otherwise stated, the experiments were performed using an Ag/AgCl saturated with KCl reference electrode. It was separated from the cell by a salt bridge containing the same electrolyte as in the cell. A Pt pseudoreference electrode was also employed to avoid contamination from the Ag/AgCl reference electrode. In any case, background voltammograms were recorded in the absence of ammonia to check for the presence of Cl^- or other impurities. No oxidation wave for chloride or other electroactive contaminants was ever observed. The microdisk electrodes employed were prepared by sealing wires of 5-, 10-, 25-, and 60- μm diameter, directly in glass. The effective electrode radii of the exposed microdisks were calculated with eq 5²¹ after recording the steady-state limiting currents in a 1 mM

$$I_d = 4nFDca \quad (5)$$

ferrocene solution in acetonitrile ($D = 2.5 \times 10^{-5} \text{ cm}^2 \text{ s}^{-1}$),²² where I_d is the diffusion-controlled limiting current and a the radius of the microdisk; the other symbols have their usual meaning. The electrode radii measured electrochemically differed by no more than 10% with respect to those determined by optical inspection with an inverted microscope (Litze Wetzlar). Linear sweep voltammetric experiments were controlled by a PAR 175 or by a Hi-Tek PPR1 function generator. A Keithley 428 picoammeter and a homemade current follower were used to measure the current, and data were plotted with a Hewlett-Packard 7045 B X–Y recorder.

To approach steady-state diffusion-limiting conditions with microelectrodes, a scan rate, ν , of 5 mV s^{-1} was employed in all the experiments. In fact, the parameter²³ $p = (nF\nu a^2/DRT)^{1/2}$ ranged from 0.016 for a 2.5- μm radius to 0.42 for a 30- μm radius using $T = 298 \text{ K}$ and $D \sim 10^{-5} \text{ cm}^2 \text{ s}^{-1}$. Under these conditions, the diffusion-limiting current should not exceed the steady-state value by more than 1% for the smallest electrode and less than 10% for the largest microdisk.

The steady-state limiting current was evaluated at a fixed potential within the potential range corresponding to the plateau, assuming as the baseline that drawn from the residual current recorded before the onset of the wave. All steady-state current data points are mean values of at least three replicates (the relative standard deviation was $\sim 3\%$).

(16) Martell, A. E.; Smith, R. M. *Critical Stability Constants*; Plenum Press: New York, 1981.

(17) Lopez de Mishima, B. A.; Lescano, D.; Molina Holgado, T.; Mishima, H. T. *Electrochim. Acta* **1998**, *43*, 395–404 and references therein.

(18) Donten, M.; Hyk, W.; Wojciech, H.; Ciszewska, M.; Stojek, Z. *Electroanalysis* **1997**, *9*, 751–754.

(19) de Voys, A. C. A.; Mrozek, M. F.; Koper, M. T. M.; van Santen, R. A.; van Veen, J. A. R.; Weaver, M. J. *Electrochem. Commun.* **2001**, *3*, 293–298.

(20) de Voys, A. C. A.; Koper, M. T. M.; van Santen, R. A.; van Veen, J. A. R. *J. Electroanal. Chem.* **2001**, *506*, 127–137.

(21) Saito, Y. *Rev. Polarogr.* **1968**, *15*, 177.

(22) Adams, R. N. *Electrochemistry at solid electrodes*; Dekker: New York, 1969; p 193.

(23) Aoki, K.; Akimoto, K.; Tokuda, K.; Matsuda, H.; Osteryoung, J. J. *Electroanal. Chem.* **1984**, *171*, 219–230.

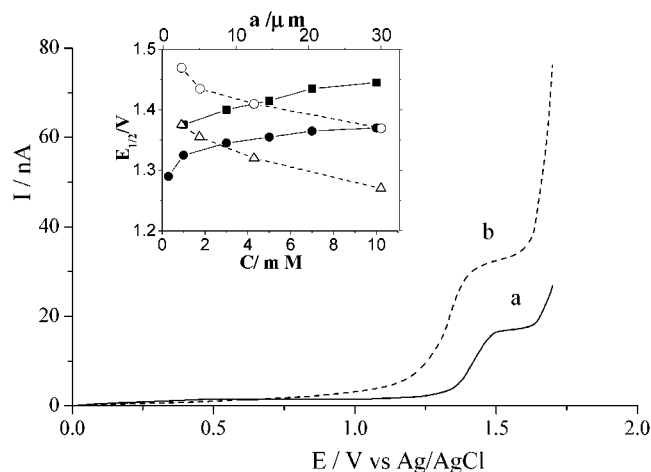


Figure 1. Steady-state voltammograms recorded at 5 mV s^{-1} with a $12.5\text{-}\mu\text{m}$ -radius gold microdisk in (a) 1.70 mM NH_3 and (b) 1.5 mM NaOH solutions and 0.1 M NaClO_4 . Inset: Half-wave potential versus radius (open symbols) and concentration (filled symbols) for NH_3 (○, ■) and NaOH (△, ●) solutions.

Theoretical steady-state limiting currents under various conditions were obtained by digital simulation. The mechanism based on reactions 1 and 2 was simulated with DigiSim (Version 3.0, Bioanalytical Systems). Since this software permits only one-electron heterogeneous processes with a 1:1 stoichiometry, and because the steady-state limiting current was the only parameter that needed to be predicted, reactions 1 and 2 was treated as a CE mechanism with an overall one-electron-transfer process.

RESULTS AND DISCUSSION

Figure 1 (trace a) shows a typical steady-state voltammogram for a solution containing 1.7 mM NH_3 and 0.1 M NaClO_4 , recorded at 5 mV s^{-1} with a $12.5\text{-}\mu\text{m}$ -radius gold microdisk, over a positive potential window large enough to include the solvent discharge. For comparison, Figure 1 (trace b) includes the wave recorded in a 1.5 mM NaOH solution with the same microelectrode and at the same scan rate. Either voltammogram displays a main oxidation wave at $\sim 1.4 \text{ V}$ and a small broad peak around $0.4\text{--}0.5 \text{ V}$. Voltammetric waves similar to that in Figure 1a were obtained from solutions containing ammonia over a range of concentrations and with electrodes having different radii. The position of the main wave depended on both ammonia concentration and electrode radius. In particular, the half-wave potential $E_{1/2}$ shifted toward more positive potentials when the electrode radius was decreased or the ammonia concentration increased (see inset in Figure 1). Similar trends for the wave position were observed in NaOH-containing solutions (also included in Figure 1). In this case, the waves recorded at about 1.4 and $0.4\text{--}0.5 \text{ V}$ were respectively assigned to the diffusion-controlled oxidation of OH^- and to the formation of gold oxides at the electrode surface.¹⁵

Figure 1 indicates that the main wave was significantly lower in the ammonia-containing solutions than in NaOH solutions for the same given concentration and electrode radius. A similar current decrease was observed when the steady-state voltammogram recorded for a weak monoprotic acid was compared with that recorded for a strong acid, with the same microelectrode and in two solutions each containing the same acid concentration.^{6,9} The current decrease observed with the weak acid was related to

Table 1. Linear Equations for Current against Radius Plots at Different Analytical Concentrations of Ammonia

CNH_3/mM	linear equations	r
1.0	$I_d (\text{nA}) = -0.33 + 0.87a (\mu\text{m})$	0.999
3.0	$I_d (\text{nA}) = -1.72 + 2.80a (\mu\text{m})$	0.999
5.0	$I_d (\text{nA}) = -1.91 + 4.57a (\mu\text{m})$	0.999
7.0	$I_d (\text{nA}) = -2.67 + 6.24a (\mu\text{m})$	0.999
10	$I_d (\text{nA}) = -4.63 + 8.89a (\mu\text{m})$	0.999

the occurrence of the CE mechanism; it is therefore tempting to invoke this reaction scheme, via the hydroxide ion oxidation, for the large oxidation wave observed in the ammonia solutions.

As mentioned above, it has been reported^{19,20} that conventional gold electrodes anodized in aqueous solutions containing ammonia at concentrations of ≥ 0.1 and 1 M NaOH produced an oxidation wave at a potential above 0.9 V , but $100\text{--}200 \text{ mV}$ (depending on the experimental conditions) less positive than that shown in Figure 1a. In this case, the oxidation process was attributed to the electrodisolution of gold to form a gold–ammonia complex (see reaction 4), along with the formation of some N_2O . Thus, the above results and considerations suggest that the main wave shown in Figure 1a may be due to the oxidation of hydroxide ions. The dissolution of gold to yield gold–ammonia complexes or the simultaneous occurrence of both CE and complexation processes cannot be excluded a priori, as the kinetics of the processes at the microelectrode may be different from those observed at conventional electrodes.

To determine which process is responsible for the wave observed in Figure 1a, the dependence of the wave height on electrode radius and concentration of both supporting electrolyte and ammonia was examined in detail.

Effect of Radius and Supporting Electrolyte. A series of measurements was carried out in solutions containing a fixed concentration of NH_3 and 0.1 M NaClO_4 as supporting electrolyte and with several microelectrodes having radii over the range $2.5\text{--}30 \mu\text{m}$. In all cases, the waves were well shaped and the steady-state limiting current displayed an apparent linearity against electrode radius. Table 1 shows the linear equations obtained by regression analysis of the experimental data recorded at different analytical concentrations of ammonia. These results appear to suggest that the process is under diffusion control.

A series of measurements was also carried out using a gold microelectrode, $12.5\text{-}\mu\text{m}$ radius, in solutions containing a fixed concentration of NH_3 with no deliberately added or little supporting electrolyte. Figure 2 shows typical voltammograms recorded under these conditions. In the solution with no deliberately added electrolyte, the wave displayed a small broad anodic peak (see Figure 3, trace a). This was particularly evident when the background conductivity of pure water was very low (i.e., $1.5 \mu\text{S cm}^{-1}$). However, when electrolyte was added (in small quantity or in excess) to the solution, the expected sigmoidal shape was always observed (Figure 2, traces b and c). The small peak is probably due to the reversible adsorption of NH_3 at the electrode surface,^{19,20} a phenomenon that might be enhanced by the lack of electrolyte. The key finding shown in Figure 2 is that, in absence of supporting electrolyte, the steady-state limiting current is larger than that with either little added or excess supporting electrolyte.

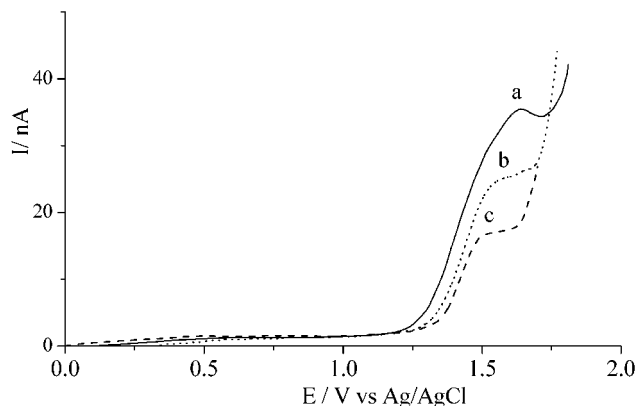


Figure 2. Steady-state voltammograms recorded at 5 mV s^{-1} with a $12.5\text{-}\mu\text{m}$ -radius gold microdisk in 2.0 mM NH_3 solutions containing (a) no added electrolyte, (b) 0.032 mM , and (c) 0.1 M NaClO_4 .

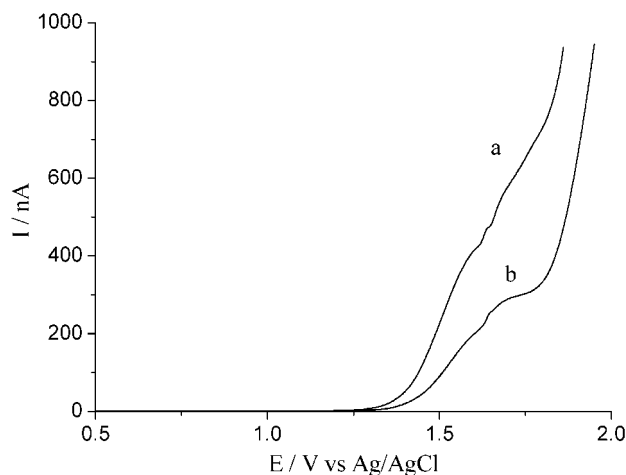


Figure 3. Steady-state voltammograms recorded at 5 mV s^{-1} with a $13\text{-}\mu\text{m}$ -radius gold microdisk in 0.1 M NaClO_4 solutions containing (a) 0.70 and (b) 0.2 M NH_3 .

The current increase in poor supporting electrolyte solutions is indicative of a migration contribution to the mass transport.^{24,25} Since migration occurs when the electroactive species is charged, the above results suggest that the electrode process should involve a negatively charged species, the working electrode being positively charged.²⁴

The ratios (I_{lm}/I_d) of the limiting current with no added or little electrolyte (I_{lm}) to the diffusion-limiting current determined for different "support ratios" ρ (that is, the ratio of the supporting electrolyte to the bulk concentration of the reactant) were 1.92, 1.70, 1.41, and 1.22, respectively, for no deliberately added electrolyte, and for ρ equal to 0.001, 0.016, and 0.1. These values are similar to those found for the reduction of weak acids under similar conditions.^{3,26} From this point of view, the voltammetric behavior observed here for the weak base parallels that found for the weak acids. Thus, by analogy, it can be concluded that the electrode process investigated here involves the one-electron oxidation of a singly charged reactant that produces a neutral species.^{3,24,26}

Effect of Ammonia Concentration. The effect of varying the analytical concentration (C_{NH_3}) of ammonia on the voltammograms was investigated in solutions at constant ionic strength (0.1 M NaClO_4). The voltammograms were similar to that shown in Figure 1a up to $C_{\text{NH}_3} = 10 \text{ mM}$. At higher concentrations, the wave became rather drawn out and split as shown in Figure 3, the second wave occurring at more positive potentials. A wave split was also observed in NaOH solutions,¹⁵ and this was attributed to the oxidation of OH^- on gold surfaces coated with different oxide films.¹⁵ Here, the wave split might also be due to the occurrence of the electrode processes 2 and 4, the latter being evident at relatively large concentrations of ammonia.^{19,20} However, on the basis of previous literature reports, this hypothesis could be ruled out because the complexation reaction coupled with the heterogeneous electron transfer should in principle occur at less positive potentials.^{27,28}

The steady-state limiting current against ammonia concentration plots over the range $0.1\text{--}10 \text{ mM}$, where a single wave was apparent, were in general linear. For instance, the linear regression analysis of the experimental data yielded $I_d \text{ (nA)} = 0.58 + 3.75 C_{\text{NH}_3} \text{ (mM)}$ (correlation coefficient $r = 0.999$) and $I_d \text{ (nA)} = -0.62 + 10.1 C_{\text{NH}_3} \text{ (mM)}$ ($r = 0.999$) for the 5- and $13\text{-}\mu\text{m}$ gold microdisks, respectively. These results contrast with those observed for weak acids, where in general the steady-state limiting current was not a linear function of the analytical concentration of the acid.^{6,9} In fact, it was shown that, for monoprotic weak acids, the steady-state limiting current depended in a rather complex fashion on the dissociation constant of the weak acid, the diffusion coefficient of the diffusing species, and on the analytical concentration of the acid itself.⁶ Moreover, the steady-state limiting current strongly depended on whether the chemical reaction was fast or under kinetic control. In general, a fast chemical equilibrium was found to occur for a weak acid whose dissociation constant is larger than 1×10^{-6} .⁶ For instance, a fast equilibrium was found to occur for the reduction process of acetic acid whose dissociation constant is $\sim 2 \times 10^{-5}$ at 0.1 M ionic strength.⁶ Therefore, for NH_3 , a fast dissociation equilibrium should also apply. These aspects will be addressed in the next paragraph.

Comparison of Experimental Data with Theoretical Prediction. To discern among the different electrode processes the one responsible for the oxidation wave in ammonia solutions, three different theoretical approaches were employed to predict the steady-state limiting current values.

The theoretical steady-state current for a pure second-order CE mechanism, via the oxidation of OH^- (that is, a reaction mechanism of the type 1–2), was determined by digital simulation. The simulation was performed under the assumption that the electrode process 2 was always irreversible. Moreover, because they were available in the literature,²⁹ $k_f = 5.0 \times 10^5 \text{ s}^{-1}$ and $k_b = 2.8 \times 10^{10} \text{ M}^{-1}\text{s}^{-1}$ were employed, respectively, for the forward and backward kinetic constants of reaction 3. With these kinetic constant values, and for the sake of data consistency, the equilibrium constant $K_b = k_f/k_b = 1.8 \times 10^{-5}$ was employed. Since most measurements were carried out in solutions at 0.1 M ionic

(24) Myland, J. C.; Oldham, K. B. *J. Electroanal. Chem.* **1993**, *347*, 49–91.

(25) Ciszowska, M.; Stojek, Z. *J. Electroanal. Chem.* **1999**, *466*, 129–143 and references therein.

(26) Xie, Y.; Liu, T. Z.; Osteryoung, J. G. *Anal. Chem.* **1996**, *68*, 4124–4129.

(27) Stojek, Z.; Osteryoung, J. G. *Anal. Chem.* **1988**, *60*, 131–136.

(28) Baldo, M. A.; Daniele, S.; Mazzocchin, G. A. *Anal. Chim. Acta* **1997**, *340*, 77–87.

(29) Eigen, M.; Schon, J. Z. *Elektrochem.* **1955**, *59*, 483.

strength where a larger dissociation constant is reported in the literature,¹⁶ a series of simulations were also performed using $K_b = 3.02 \times 10^{-5}$, with k_b the same value as above (that is, a diffusion-limited value, as is typical for the recombination reactions in acid base equilibria),³⁰ and $k_f = 8.46 \times 10^5 \text{ s}^{-1}$ for the sake of data consistency. The data simulated using the two different sets of kinetic and thermodynamic constants will be referred as SIM1 and SIM2, respectively. The diffusion coefficient of hydroxide ions $D_{\text{OH}^-} = 4.62 \times 10^{-5} \text{ cm}^2 \text{ s}^{-1}$ at 25 °C and at 0.1 M ionic strength was also taken from the literature.¹⁰ Since rather different values have been reported for the diffusion coefficient of ammonia D_{NH_3} (ranging from 2.1×10^{-5} to $1.75 \times 10^{-5} \text{ cm}^2 \text{ s}^{-1}$),^{17,18} we decided to calculate it from the known mobility of NH_4^+ at infinite dilution, assuming $D_{\text{NH}_4^+} = D_{\text{NH}_3}$, and making a correction for both the ionic strength and viscosity of the medium.^{11,31} In this way, a value of $1.80 \times 10^{-5} \text{ cm}^2 \text{ s}^{-1}$ was calculated at 0.1 M NaClO_4 . It compares well with that reported in ref 17.

If the chemical equilibrium of ammonia that precedes the electron-transfer process is fast, the following equation should apply:⁶

$$I_{\text{d}} = 4nFa(D_{\text{OH}^-}[\text{OH}^-] + D_{\text{NH}_3}[\text{NH}_3]) \quad (6)$$

where $[\text{OH}^-]$ and $[\text{NH}_3]$ are equilibrium bulk concentrations of hydroxide ion and ammonia, respectively. This equation was derived, by analogy with that for weak acids, by resorting to the apparent diffusion coefficient of the base (that is, the mole fraction average of OH^- and NH_3 present in the bulk solution at equilibrium).^{6,32}

To predict the steady-state limiting current (I_{dc}) for the occurrence of reaction 4, the diffusion layer model to a microdisk²⁷ for the oxidation of gold to Au(I) , coupled with the complex formation, was applied. Moreover, the influence of chemical reaction 3 coupled with reaction 4 was taken into account by using the apparent diffusion coefficient D_{app} defined as $D_{\text{app}}C_{\text{NH}_3} = (D_{\text{OH}^-}[\text{OH}^-] + D_{\text{NH}_3}[\text{NH}_3])$. From this simplified treatment and under the assumption that reaction 4 is fast, one obtains

$$I_{\text{dc}} = 4nFD_{\text{app}}C_{\text{NH}_3}a/p \quad (7)$$

where p is the number of ammonia molecules involved in the gold complex. $p = 2$ was always considered here.³³ This simply implies that the steady-state limiting current calculated by eq 7 is half of that calculated by eq 6.

The theoretical data calculated with the three different procedures (simulation, eq 6, and eq 7) presented above are displayed in Figures 4 and 5, which show current against concentration data for different electrode radii. From these figures, the following remarks can be made. The data obtained by simulation either with the SIM1 (Figure 4) or SIM2 (Figure 5) parameters and those

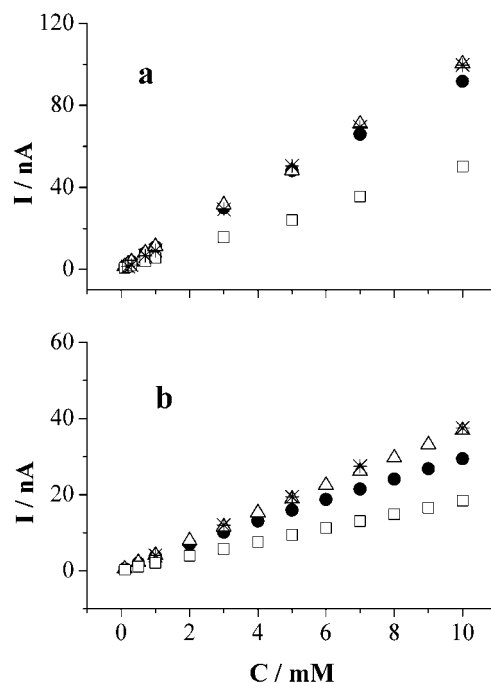


Figure 4. Theoretical and experimental steady-state limiting current versus the concentration of NH_3 for (a) 13- and (b) 5- μm -radius gold microdisks. Theoretical values obtained by (●) simulation with the SIM1 parameters, (Δ) eq 6, and (□) eq 7; (*) experimental values.

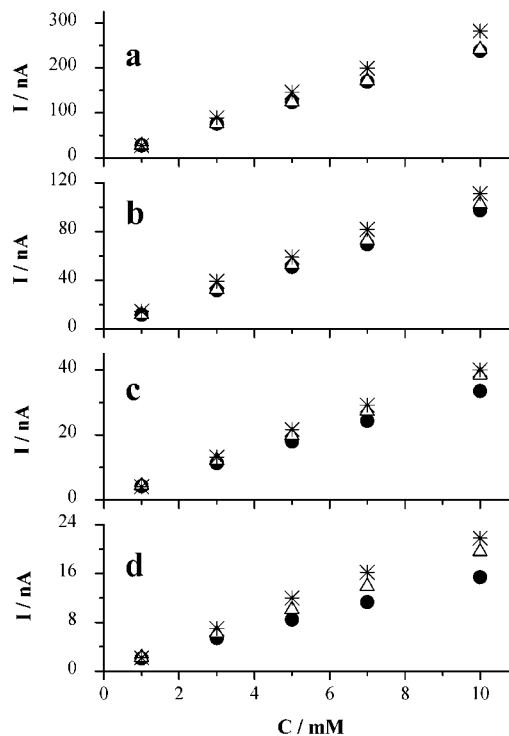


Figure 5. Theoretical and experimental steady-state limiting current versus the concentration of NH_3 for (a) 32-, (b) 13-, (c) 5-, and (d) 2.6- μm -radius gold microdisks. Theoretical values obtained by (●) simulation with the SIM2 parameters and (Δ) eq 6; (*) experimental values.

calculated by eq 6 differ to an extent that depends on both the electrode radius and the ammonia concentration. In general, the agreement between the data obtained by simulation and those calculated by eq 6 is better for larger electrodes and smaller

(30) Bell, R. P. *The Proton in Chemistry*; Methuen & Co., Ltd.: London, 1959; p 109.

(31) Jaworski, A.; Osteryoung, J. G.; Donten, M.; Stojek, Z. *Anal. Chem.* **1999**, *71*, 3853–3861.

(32) Carofiglio, T.; Magno, F.; Lavagnini, I. *J. Electroanal. Chem.* **1994**, *373*, 11–17.

(33) Trejo, G.; Gil, A. F.; Gonzalez, I. *J. Electrochem. Soc.* **1995**, *142*, 3404–3408.

ammonia concentrations. Moreover, for similar electrode radii, simulated and calculated data agree better when the SIM2 parameters are used (compare data in Figures 4 and 5b,c). This is congruent with the larger thermodynamic constant and forward kinetic constant that apply in this second case. Since for a fast equilibrium the current data obtained by simulation and calculated with eq 6 should overlap,^{6,9} the data shown in Figures 4 and 5 suggest that chemical equilibrium 3 is, to some extent, kinetically hindered for ammonia concentrations larger than 1 mM and for microelectrodes with a radius of $\leq 5 \mu\text{m}$. The maximum difference obtained between simulated and calculated data is $\sim 20\%$ for the $2.5\text{-}\mu\text{m}$ disk electrode and 10 mM NH_3 concentration level.

The experimental data shown in Figures 4 and 5, in general, either fit or are even slightly larger than those calculated by eq 6. On the contrary, the experimental data never fit those calculated by eq 7. This means that the oxidation wave occurring in ammonia solutions, over the concentration range 0.1–10 mM, can be mainly explained on the basis of a CE mechanism involving the oxidation of hydroxide ions. Moreover, for the sets of diffusive, thermodynamic, and kinetic parameters available, the chemical reaction that precedes the electron transfer is fast enough (within 8% error for a 10 mM NH_3) to support mass transport control with microelectrodes having radii of $\geq 5 \mu\text{m}$. The experimental currents, which are generally larger than those predicted by theory (especially with the smaller electrodes), could be explained by including a parallel electrode reaction besides the CE process. This probably involves ammonia itself in an oxidation that requires more than one electron per mole of ammonia, e.g., to form N_2O .^{19,20}

The data obtained here over the ammonia concentration range 0.1–10 mM allow us in any case to rule out the occurrence of reaction 4. This suggests that reaction 4 is strongly hindered at the microelectrodes. This aspect was not investigated further. With large ammonia concentrations, reaction 4 could take place but at a potential more positive than those due to the oxidation of hydroxide ions. Its effect would not be significant for the concentration range used here.

Buffer Solutions. There are practical instances in which the determination of ammonia is performed in buffered media.³⁴ To verify whether measurements could be taken under these conditions and as a preliminary study, the anodization of the gold microelectrodes was also examined in buffers made by mixing NH_3 with either NH_4ClO_4 or NH_4NO_3 . In solutions containing the salts without ammonia, no wave was ever observed before the background discharge, whereas waves with features similar to that shown in Figure 1a were recorded when NH_3 was added to the NH_4NO_3 or NH_4ClO_4 electrolyte. Experiments made by fixing the concentration of NH_4ClO_4 (or NH_4NO_3) and the electrode radius, but varying the NH_3 concentration, indicated that the steady-state limiting current was proportional to the analytical concentration of ammonia. For instance, in a 10 mM NH_4ClO_4 solution and with a $5\text{-}\mu\text{m}$ -radius gold microdisk, the steady-state limiting current was proportional to the analytical concentration of ammonia over the range 1–10 mM. The linear regression analysis of the experimental data yielded a slope of $3.30 \times 10^{-3} \text{ A mol}^{-1} \text{ cm}^{-3}$ for a correlation coefficient of 0.999. Since ammonia

is the prevailing species in these buffers, eq 8 was derived from eq 6:

$$I_{\text{d}} = 4nFD_{\text{NH}_3}aC_{\text{NH}_3} \quad (8)$$

From the latter expression and the above experimental slope, a diffusion coefficient value of $1.71 \times 10^{-5} \text{ cm}^2 \text{ s}^{-1}$ was calculated for ammonia. This value agrees within 5% with that obtained above from mobility data at infinite dilution. These results once again parallel those reported for weak acids in buffers,¹² where a simple relationship similar to eq 8 could be derived. These preliminary results suggest therefore that, even in buffer solutions, the analytical concentration of ammonia can be determined by a simple relationship obtained for the CE mechanism involving the hydroxide ion oxidation.

CONCLUSIONS

Based on the results reported here, one can conclude that the oxidation wave that appears in ammonia containing solutions over the concentration range 0.1–10 mM is congruent with a CE process involving the oxidation of hydroxide ion to oxygen. In fact, the measurements carried out in the absence or with small amounts of deliberately added supporting electrolyte are consistent with a mechanism involving a charged species that oxidizes to a neutral. The electroactive species, i.e., the hydroxide ion, is produced from a fast chemical equilibrium in solutions containing NH_3 at $\leq 5 \text{ mM}$ and with microelectrodes with a radius of $\geq 5 \mu\text{m}$. The largest kinetic hindering was found with the $2.5\text{-}\mu\text{m}$ disk electrode where simulated data differ by as much as 22% from those obtained by eq 6.

The CE process seems to be complicated by a parallel chemical reaction that probably involves, to a limited extent, the direct oxidation of ammonia itself. The results and conclusion of this study agree with those reported in refs 19 and 20 where, from surface-enhanced Raman spectroscopy measurements, it is concluded that gold, unlike other metals such as Pt and Ir, is inactive in the selective oxidation of ammonia to N_2 . However, it is likely that some N_2O is formed^{19,20} when the kinetic hindering of the CE process is relatively high; this would explain that the experimental currents found are larger than those expected for an overall one-electron-oxidation reaction. Our findings are not consistent with the enhanced electrodisolution of gold in the presence of ammonia to yield gold–ammonia complexes.^{19,20} In fact, if this mechanism were responsible for the wave shown in Figure 1a (or Figure 3), it should not have been affected by migration, as only molecular ammonia would be involved in the electrode process. Moreover, if reaction 4 were, even in part, responsible for the oxidation wave in Figure 1a, rather lower steady-state limiting current should have been observed.

A final consideration of the linearity observed for the current against concentration plots is required. Comparing once again the behavior of a weak base and of a weak acid, the reason for the linearity observed between steady-state limiting current and concentration is due to the fact that the diffusion coefficients of the hydroxide ions and ammonia, which are the diffusing species in equilibrium, are not so much different from one another (the diffusion coefficient of the hydroxide ion is less than 3 times greater than that of NH_3). In the case of weak acids, the diffusion

coefficient of hydrogen ions is 1 order of magnitude greater than that of the undissociated acid.^{6,9} Moreover, over the concentration range 1–10 mM, ammonia is the prevailing species at equilibrium and it therefore substantially controls the rate and mechanism of the reaction. The observed linearity between current and concentration is very useful from an analytical point of view since the evaluation of the analytical concentration of ammonia can be made straightforwardly by, for instance, the standard addition

(34) Strehlitz, B.; Grundig, B.; Kopinke, H. *Anal. Chim. Acta* **2000**, *403*, 11–23.

(35) Daniele, S.; Baldo, M. A.; Bragato, C.; Mori, G.; Gianneto, M. *Anal. Chim. Acta* **2001**, *432*, 27–37.

procedure. This is at variance with the case of weak acids, where in some cases the determination of the analytical concentration by voltammetry or amperometry may be difficult.³⁵

ACKNOWLEDGMENT

Financial support by MURST, Rome (Piano “servizi al cittadino ed al territorio” cluster C 22, Progetto 20) is gratefully acknowledged.

Received for review January 18, 2002. Accepted April 24, 2002.

AC025530N